AFRL-PR-WP-TR-2000-2066

AN INVESTIGATION IN FINITE ELEMENT THEORY OF SHEAR LOCKED ELEMENTS

LT BRIAN BEACHKOFSKI

AFRL/PRTC
1950 5TH STREET
WRIGHT-PATTERSON AFB, OH 45433-7251

JUNE 2000

FINAL REPORT FOR OCT 1999 – FEB 2000

PROPULSION DIRECTORATE
AIR FORCE RESEARCH LABORATORY
AIR FORCE MATERIEL COMMAND
WRIGHT-PATTERSON AIR FORCE BASE OH 45433-7251

Form SF298 Citation Data

Report Date ("DD MON YYYY") 01-06-2000	Report Type N/A	Dates Covered (from... to) ("DD MON YYYY") 01-10-1999 01-02-2000

Title and Subtitle An Investigation In Finite Element Theory of Shear Locked Elements	**Contract or Grant Number**
	Program Element Number
Authors Beachkofski, Brian	**Project Number**
	Task Number
	Work Unit Number
Performing Organization Name(s) and Address(es) AFRL/PRTC 1950 5th St. Wright-Patterson AFB, OH 45433-7251	**Performing Organization Number(s)**
Sponsoring/Monitoring Agency Name(s) and Address(es) Propulsion Directorate Air Force Research Laboratory Air Force Materiel Command Wright-Patterson AFB, OH 45433-7251	**Monitoring Agency Acronym** AFRL/PRTC
	Monitoring Agency Report Number(s)

Distribution/Availability Statement
Approved for public release, distribution unlimited

Supplementary Notes

Abstract
This report shows the theoretical background for some of the problems associated with shear loaded beams using the finite element method. The report develops the theory behind both shell and brick elements on a reduced order by using beam and membrane elements. The cause of the shear-locking phenomenon is presented, as are common methods of avoiding these effects. The two presented methods of defeating shear locking are adding a bubble mode to an element, and creating the stiffness matrix with reduced order Gaussian integration. The reasoning behind each solution to the locking problem is explained and demonstrated both mathematically and through solutions to an example problem. After the validity of the particular elements is verified, general guidelines for which element type should be used are given.

Subject Terms
Finite Element; Shear Locking; Bubble Modes; Reduced Integration

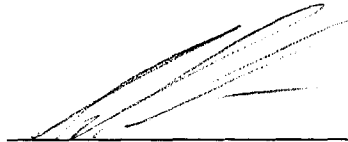| **Document Classification** unclassified	**Classification of SF298** unclassified

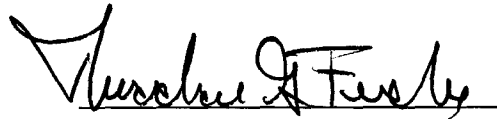| Classification of Abstract unclassified	Limitation of Abstract unlimited
Number of Pages 41	

NOTICE

Using Government drawings, specifications, or other data included in this document for any purpose other than Government procurement does not in any way obligate the U.S. Government. The fact that the Government formulated or supplied the drawings, specifications, or other data does not license the holder or any other person or corporation; or convey any rights or permission to manufacture, use, or sell any patented invention that may relate to them.

This report is releasable to the National Technical Information Service (NTIS). At NTIS, it will be available to the general public, including foreign nations.
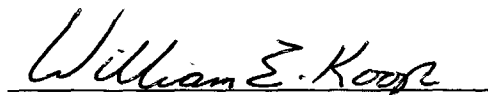
THIS TECHNICAL REPORT HAS BEEN REVIEWED AND IS APPROVED FOR PUBLICATION.

BRIAN K. BEACHKOFSKI, 1Lt, USAF
Project Engineer
Components Branch
Turbine Engine Division
Propulsion Directorate

THEODORE G. FECKE
Chief, Components Branch
Turbine Engine Division
Propulsion Directorate

WILLIAM E. KOOP
Chief of Technology
Turbine Engine Division
Propulsion Directorate

Do not return copies of this report unless contractual obligations or notice on a specific document requires its return.

REPORT DOCUMENTATION PAGE			Form Approved OMB No. 0704-0188

Public reporting burden for this collection of information is estimated to average 1 hour per response, including the time for reviewing instructions, searching existing data sources, gathering and maintaining the data needed, and completing and reviewing the collection of information. Send comments regarding this burden estimate or any other aspect of this collection of information, including suggestions for reducing this burden, to Washington Headquarters Services, Directorate for Information Operations and Reports, 1215 Jefferson Davis Highway, Suite 1204, Arlington, VA 22202-4302, and to the Office of Management and Budget, Paperwork Reduction Project (0704-0188), Washington, DC 20503.

1. AGENCY USE ONLY *(Leave blank)*	2. REPORT DATE JUNE 2000	3. REPORT TYPE AND DATES COVERED FINAL REPORT FOR OCT 1999 - FEB 2000

4. TITLE AND SUBTITLE AN INVESTIGATION IN FINITE ELEMENT THEORY OF SHEAR LOCKED ELEMENTS	5. FUNDING NUMBERS C IN-HOUSE PE 62203 PR 3066 TA 12 WU TJ
6. AUTHOR(S) LT BRIAN BEACHKOFSKI	

7. PERFORMING ORGANIZATION NAME(S) AND ADDRESS(ES) AFRL/PRTC 1950 5th STREET WRIGHT-PATTERSON AFB, OH 45433-7251	8. PERFORMING ORGANIZATION REPORT NUMBER

9. SPONSORING/MONITORING AGENCY NAME(S) AND ADDRESS(ES) PROPULSION DIRECTORATE AIR FORCE RESEARCH LABORATORY AIR FORCE MATERIEL COMMAND WRIGHT-PATTERSON AFB, OH 45433-7251 POC: LT BRIAN BEACHKOFSKI, AFRL/PRTC, 937-255-4826	10. SPONSORING/MONITORING AGENCY REPORT NUMBER AFRL-PR-WP-TR-2000-2066

11. SUPPLEMENTARY NOTES

Available on CD

12a. DISTRIBUTION AVAILABILITY STATEMENT APPROVED FOR PUBLIC RELEASE, DISTRIBUTION UNLIMITED.	12b. DISTRIBUTION CODE

13. ABSTRACT *(Maximum 200 words)*

This report shows the theoretical background for some of the problems associated with shear loaded beams using the finite element method. The report develops the theory behind both shell and brick elements on a reduced order by using beam and membrane elements. The cause of the shear-locking phenomenon is presented, as are common methods of avoiding these effects. The two presented methods of defeating shear locking are adding a bubble mode to an element, and creating the stiffness matrix with reduced order Gaussian integration. The reasoning behind each solution to the locking problem is explained and demonstrated both mathematically and through solutions to an example problem. After the validity of the particular elements is verified, general guidelines for which element type should be used are given.

14. SUBJECT TERMS Finite Element, Shear Locking, Bubble Modes, Reduced Integration	15. NUMBER OF PAGES 41
	16. PRICE CODE

17. SECURITY CLASSIFICATION OF REPORT UNCLASSIFIED	18. SECURITY CLASSIFICATION OF THIS PAGE UNCLASSIFIED	19. SECURITY CLASSIFICATION OF ABSTRACT UNCLASSIFIED	20. LIMITATION OF ABSTRACT SAR

Standard Form 298 (Rev. 2-89) (EG)
Prescribed by ANSI Std. 239.18
Designed using Perform Pro, WHS/DIOR, Oct 94

TABLE OF CONTENTS

LIST OF FIGURES

SECTION 1

INTRODUCTION

The finite element method is a very simple way to find many things including stresses and deflections in a structure. The meshing choice, element formulation and density determine the results for a given structure. Additionally, computational costs are very sensitive to the degrees of freedom in the mesh. Beyond those choices, the integration scheme and the integration network also have a large influence in the results. These sensitivities are exaggerated in certain load cases, especially in a shear or bending dominated loading conditions.

This report is a simple introduction to these factors and the mathematical theory behind them. The theory behind the report is that an analyst who understands when, as well as why each problems occurs, will be able to judge when it is best to select different options in the analysis.

1.1   Background

The finite element method is based on using the constitutive laws and stress-strain relationships for a given object to approximate the stress field throughout the object. Depending on the element this is done in different ways. Each element is given different degrees of freedom that affect how the energy of the material is represented.

However the energy is represented, the solution method is similar. The potential energy is calculated by subtracting the work done by the applied loads from the strain energy of the material. Setting the variation in the potential energy to zero defines the equilibrium position. By creating as many equations as there are degrees of freedom, the value of each degree of freedom can be found by solving the simultaneous equations. The general principle is shown below.

$$\pi = V - W$$
$$\pi = \underline{u}^T K \underline{u} - \underline{u}^T \underline{F}$$
$$\delta\pi = \delta\underline{u}^T K \underline{u} - \delta\underline{u}^T \underline{F}$$
$$\delta\pi = 0 = \delta\underline{u}^T \left[K\underline{u} - \underline{F} \right]$$
$$K\underline{u} = \underline{F}$$
$$\underline{u} = K^{-1} \underline{F}$$

π – Total potential energy
V – Strain energy
W – Work
K – Stiffness matrix
F – Force vector
u – Nodal displacements
δ – First Variation

The key to this is that the work must be expressed as forces applied at discrete points on the structure and that the strain energy can be expressed as some stiffness relationship multiplied by a combination of two displacements at the nodes. Fortunately, the constitutive laws and strain displacement relationships most commonly used apply exactly to this form.

There are some flaws with the method. The constitutive laws, in certain cases, create a situation where the solution to the system of equations does not converge to the correct answer. There are a variety of simple solutions to rectify the problem, either based on changing the properties of the element, or by changing the way the stiffness matrix is formulated.

1.2   Scope

This report will use as an example a cantilevered beam with a tip shear load shown in Figure 1. This condition was chosen because it is relatively easy to find a closed form solution to the deflection and that the problems in the elements will be easily identified. Additionally, the cantilevered beam is an elementary model for many objects in structural analysis, from wings to buildings.
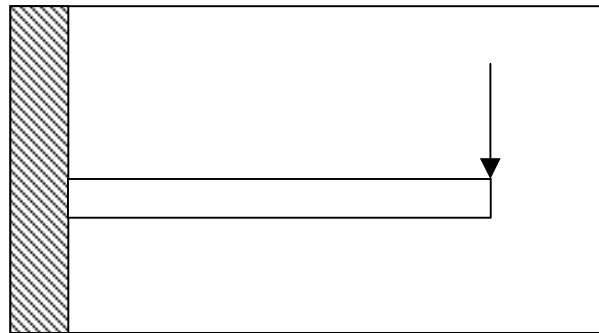
Figure 1. Test Configuration.

The elements that are examined are shell and brick elements, both with nodes only at the corners. During the discussions the equations will be developed for a two-dimensional version of the element instead of the three-dimensional ones used in the actual analysis. This is done only to significantly reduce the size of the problems. The mathematics is the same for the three-dimensional case, but the three-dimensional case would have over twice the degrees of freedom.

This report is intended only as an introduction to the mathematical reasoning behind the finite element method. It is intended only to allow the user to decide when it is justified to use a given mesh density, a particular element, or integration technique. Hopefully it will allow an analyst to better balance the benefits of a highly refined mesh and the necessity to reduce computational costs.

SECTION 2
EXACT SOLUTION

This particular test configuration was chosen because it not only produces the phenomenon that we want to explore, but because it is relatively easy to find the exact form of the solution. This will prepare a baseline to which the finite element models can be compared.

Two different solutions are examined. The first is the deflection solution, which accounts for both the bending deformation and the shear deformation. This method uses the variation of total potential energy to determine the governing equations. The second is the frequency analysis, which uses Euler-Bernoulli assumptions. These assumptions should be valid for the natural frequencies because natural frequencies are independent of loading conditions, so the shear loading should not matter as much in the deflection case. Further, the beam is a long slender beam so the Euler-Bernoulli assumptions should be valid under any loading condition. This method uses the summation of forces to determine an equilibrium condition.

2.1   Deformation Solution

The deflection solution includes both the bending and the shear deformation energy. The beam is isotropic and constant cross-section. The dimensions of the beam are shown in Figure 2 below. The curvature is defined as the change in rotation and the shear is defined as the difference between the slope and the rotation. The total potential energy is the bending energy and the shear energy less the work done by the tip load.
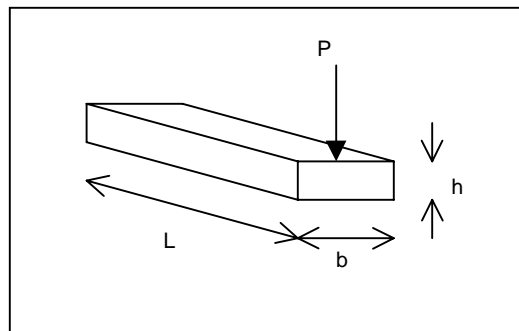
Figure 2. Dimensions of Test Beam.

There are several material properties that must also be known:

E – Young's modulus
G – Shear modulus
ν – Poisson's ratio
$\phi(x)$ – Rotation field
u(x) – Displacement field

κ – Shear stiffness
I – Moment of inertia
P – Applied tip load
π - Total potential energy

The first step is to simplify the equation by making it non-dimensional.

$$\pi = \frac{1}{2}\int_0^L EI\left(\frac{d\phi}{dx}\right)^2 dx + \frac{1}{2}\int_0^L G\kappa\left(\frac{du}{dx}-\phi\right)^2 dx - Pu\Big|_{x=L}$$

$$\eta = \frac{x}{L}$$

$$\pi = \frac{1}{2}\int_0^1 \frac{EI}{L^2}(\phi')^2 Ld\eta + \frac{1}{2}\int_0^1 G\kappa\left(\frac{u'}{L}-\phi\right)^2 Ld\eta - PL\frac{u}{L}\Big|_{\eta=1}$$

$$k = \frac{G\kappa L^2}{EI}$$

$$\frac{\pi L^2}{EI} = \frac{1}{2}\int_0^1 (\phi')^2 d\eta + \frac{1}{2}\int_0^1 \frac{G\kappa L^2}{EI}\left(\frac{u'}{L}-\phi\right)^2 d\eta - \frac{PL^2}{EI}\frac{u}{L}\Big|_{\eta=1}$$

$$p = \frac{PL^2}{EI}$$

$$\frac{\pi L^2}{EI} = \frac{1}{2}\int_0^1 (\phi')^2 d\eta + \frac{1}{2}\int_0^1 k\left(\left(\frac{u'}{L}\right)^2 - 2\phi\frac{u'}{L}+\phi^2\right)d\eta - p\frac{u}{L}\Big|_{\eta=1}$$

Then, the first variation is set to zero in order to find the equilibrium conditions. Integration by parts allows grouping on the variation of each field.

$$0 = \int_0^1\left[\phi'\delta\phi' + k\frac{u'}{L}\delta\frac{u'}{L} - k\frac{u'}{L}\delta\phi - k\phi\delta\frac{u'}{L} + k\phi\delta\phi\right]d\eta - p\delta\frac{u}{L}\Big|_{\eta=1}$$

$$0 = \int_0^1 \delta\phi\left[k\phi - \phi'' - k\frac{u'}{L}\right]d\eta + \int_0^1 \delta u\left[k\phi' - k\frac{u''}{L}\right]d\eta +$$

$$\delta u\left[k\frac{u'}{L}-k\phi - p\right]_{\eta=1} + \delta u\left[k\frac{u'}{L}-k\phi\right]_{\eta=0} + (\delta\phi)\phi'\big|_{\eta=1} + (\delta\phi)\phi'\big|_{\eta=0}$$

To set the variation to zero, each differential equation multiplied by an arbitrary variation must be equal to zero. The boundary terms multiplied by an arbitrary variation must equal zero at each boundary as well. This produces two differential equations and four boundary conditions.

$$DEs:$$

$$\frac{u''}{L} = \phi'$$

$$\phi'' = k\phi - k\frac{u'}{L}$$

$$BCs:$$

$$\phi'\big|_{\eta=1} = 0$$

$$\phi\big|_{\eta=0} = 0$$

$$\left[k\frac{u'}{L}-k\phi - p\right]_{\eta=1}$$

$$\frac{u}{L}\Big|_{\eta=0} = 0$$

We find the equilibrium positions for the unknown displacement and rotation by solving the simultaneous differential equations subjected to the boundary conditions. This produces the two equations for the solution shown below. The

equations are shown in non-dimensional form, but it would be easy to convert them to dimensional form.

$$\phi = -\frac{1}{2}p\eta^2 + p\eta$$

$$\frac{u}{L} = -\frac{1}{6}p\eta^3 + \frac{1}{2}p\eta^2 + \frac{p}{k}\eta$$

2.2   Natural Frequency

The natural frequencies are found by summing the forces and moments about a typical section of the beam shown in the figure below. The moment (M) and the shear force (V) cause stresses on the end of the section. We will employ the Euler-Bernoulli set of assumptions, which equate the slope and the rotation. Because of that, the deflection is the only field that we are attempting to solve. This is a dynamic problem, so our deflection, u, is a function of position (x) and of time (t).
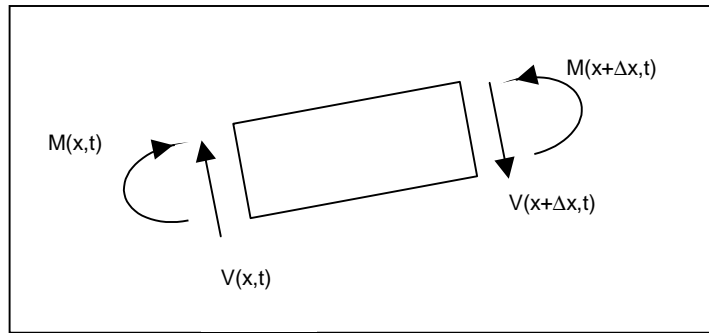
Figure 3. Typical Bending Beam Section.

First let us examine the moment equation. The Euler-Bernoulli assumptions also say that the rotational inertia is small, allowing us to equate the sum of the moments to zero. The equation is a first order approximation of the system. This means that the moment and the shear field can be looked at as a linear function across Δx. It also implies that higher order terms of Δx are approximately zero.

$$\sum M = M(x,t) + \frac{\partial M(x,t)}{\partial x}\Delta x - V(x,t)\Delta x - \frac{\partial V(x,t)}{\partial x}\Delta x^2 - M(x,t) = 0$$

$$\left(\frac{\partial M(x,t)}{\partial x} - V(x,t)\right)\Delta x = 0$$

$$V(x,t) = \frac{\partial M(x,t)}{\partial x}$$

Next we sum the forces using the same first order approximations. This time equating the sum of the forces to the mass times the acceleration of the section.

$$\sum F = V(x,t) - V(x,t) - \frac{\partial V(x,t)}{\partial x} \Delta x = \rho A \Delta x \frac{\partial^2 u}{\partial t^2}$$

$$\frac{\partial V(x,t)}{\partial x} \Delta x = -\rho A \Delta x \frac{\partial^2 u}{\partial t^2}$$

We combine the equations by differentiating the result of the moment equation.

$$\frac{\partial V(x,t)}{\partial x} = \frac{\partial^2 M(x,t)}{\delta x^2}$$

$$\frac{\partial^2 M(x,t)}{\delta x^2} = -\rho A \frac{\partial^2 u}{\partial t^2}$$

The Euler-Bernoulli assumption states that the moment is equal to the bending stiffness (EI) times the second derivative of the deflection. This comes from equating the rotation with the slope, meaning that the curvature is the second derivative of the deflection. We use this to reduce our differential equation to a single time and space dependent variable.

$$M(x,t) = EI \frac{\partial^2 u}{\partial x^2}$$

$$\frac{\partial^4 u}{\partial x^4} + \frac{\rho A}{EI} \frac{\partial^2 u}{\partial t^2} = 0$$

$$\frac{\partial^4 u}{\partial x^4} + c^2 \frac{\partial^2 u}{\partial t^2} = 0$$

Suitable boundary conditions need to be developed for this differential equation. For free vibrations we know that the free end will carry no shear load or moment. Using the earlier definitions for our shear and moments, and a fixed displacement and slope at the cantilevered end we get the following boundary conditions.

$$u(0,t) = 0 \qquad \frac{\partial^2 u(L,t)}{\partial x^2} = 0$$

$$\frac{\partial u(0,t)}{\partial x} = 0 \qquad \frac{\partial^3 u(L,t)}{\partial x^3} = 0$$

Using separation of variables, with λ being the separation constant, the deflection equation becomes:

$$\phi(x) = c_1 \sin(\beta x) + c_2 \cos(\beta x) + c_3 \sinh(\beta x) + c_4 \cosh(\beta x)$$

$$\beta^4 = \lambda^2 c^2$$

After the boundary conditions are applied, you reduce the system to two equations and two unknowns.

$$\begin{bmatrix} \sin(\beta L)+\sinh(\beta L) & \cos(\beta L)+\cosh(\beta L) \\ \cos(\beta L)+\cosh(\beta L) & -\sin(\beta L)+\sinh(\beta L) \end{bmatrix}\begin{bmatrix} c_1 \\ c_2 \end{bmatrix} = \begin{bmatrix} 0 \\ 0 \end{bmatrix}$$

To avoid the trivial solution, it is necessary to make to determinate of the matrix equal to zero. This is done by varying the values of βL. The first few values that create a zero determinate are listed below. From the time dependent portion of the separation of variables, the frequency of oscilliation was shown to be λ. Using the material properties and the relationships shown above the βL values are changed into frequencies. The units are then changed from radians per second to hertz.

βL= 1.875104		λ_1= 9.7260 Hz
βL= 4.694091		λ_2= 60.9518 Hz
βL= 7.854757		λ_3= 170.6668 Hz
βL= 10.995541		λ_4= 334.4388 Hz
βL= 14.137169		λ_5= 552.8514 Hz

By changing the orientation of the beam it is easy to find the lateral bending frequencies. Only the first bending is low enough to be relavent to the problem.

$$\lambda_{lat}= 194.5200 \text{ Hz}$$

This type of analysis will not give the torsional mode frequencies. To get those frequencies, we must look again at the typical section of the beam, seen in Figure 4.
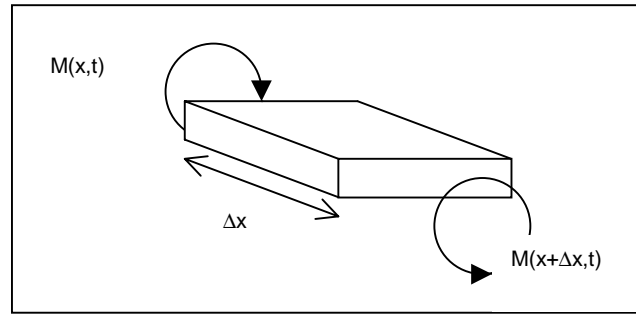
Figure 4. Typical Torsional Beam Section.

This time there are no forces and the rotations are not considered small, so the moments are set equal to polar moment multiplied by the angular acceleration.

$$\sum M = M(x,t) + \frac{\partial M(x,t)}{\partial x}\Delta x - M(x,t) = \rho \Delta x (I_{xx}+I_{yy})\frac{\partial^2 \phi}{\partial t^2}$$

$$\frac{\partial M(x,t)}{\partial x} - \rho(I_{xx}+I_{yy})\frac{\partial^2 \phi}{\partial t^2} = 0$$

The moment can also be written in the following form,

where J is the torsional stiffness of the beam. For a beam with a 10:1 aspect ratio cross-section, such as the one in the model, J is defined as below.
As in the bending case, this relationship is used to create a single field differential equation. The boundary conditions of a one fixed end and one with no moment are also translated mathmatically.

$$J = dbh^3$$
$$d = 0.313$$

Using separation of variables and the boundary conditions as in the bending case, the non-trivial solution is satisfied if λ has the following values.

$$\frac{\partial^2 \phi(x,t)}{\partial x^2} + c^2 \frac{\partial^2 \phi(x,t)}{\partial t^2} = 0$$

$$c^2 = \frac{\rho(I_{xx} + I_{yy})}{GJ}$$

$BCs:$

$$\phi(0,t) = 0$$

$$\frac{\partial \phi(L,t)}{\partial x} = 0$$

$\beta L = \pi/2$	$\lambda_1 = 89.6567$ Hz
$\beta L = 3\pi/2$	$\lambda_2 = 268.9700$ Hz
$\beta L = 5\pi/2$	$\lambda_3 = 448.2834$ Hz
$\beta L = 7\pi/2$	$\lambda_4 = 627.5968$ Hz
$\beta L = 9\pi/2$	$\lambda_5 = 806.9101$ Hz

The first ten frequencies have been calculated as:

1 bend	2 bend	1 tor	3 bend	1 lat
9.726	60.952	89.657	170.667	194.520

2 tor	4 bend	3 tor	5 bend	4 tor
268.970	334.439	448.283	552.851	627.597

To calculate the mode shapes we need to return to the shape function. Then we can vary βL from 0 to the value calculated above. We must also solve for each of the four constants that appear in the equation. Unfortunately we used some of the information to determine the frequencies, so we still have one more unknown variable than the number of equations. We can pick a unit value for one of the constants and define the other by the ratio of the two. The value of the deflection is normalized by the stiffness matrix such that the mode shape vector transposed times the stiffness matrix times the mode shape vector is equal to one. The analagous method of normalization in the exact form of the solution would be to integrate the stiffnesses times the degrees of freedom squared over the length of the beam. That is more effort than the resulting benefit would yield, so only the unnormalized results are shown in the figure below. Also the torsional modes are more difficult to show when assumed to be a part of a one-dimensional beam. Therefore, Figure 5 only shows the first three bending modes.

Figure 5. Theory Based Bending Mode Shapes.
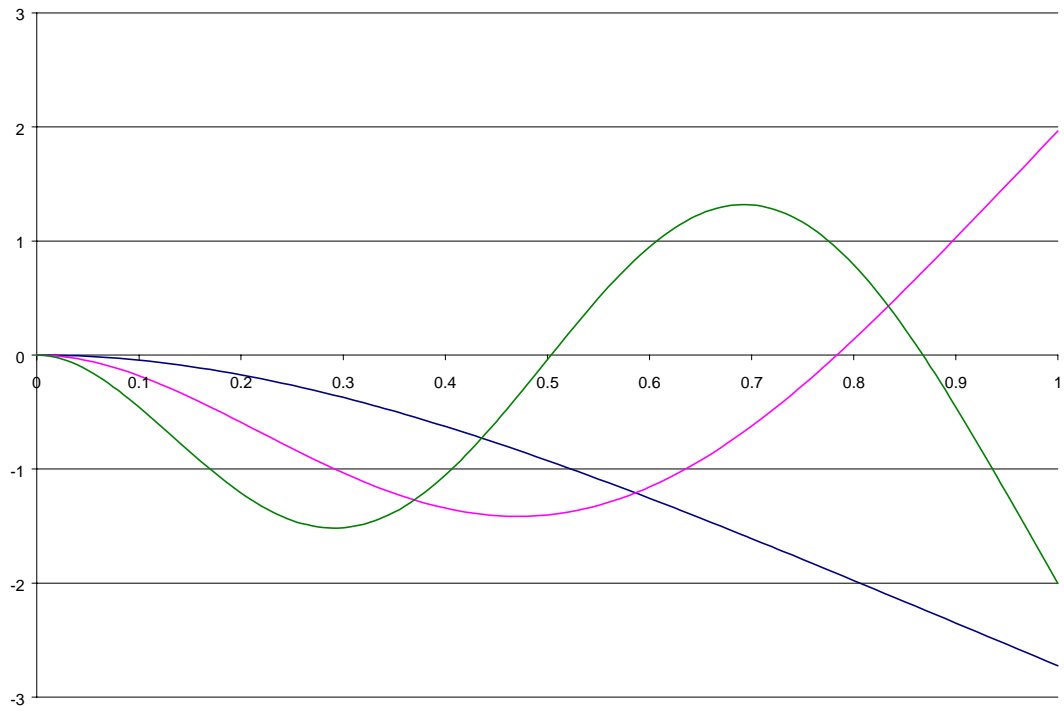
SECTION 3
SHELL ELEMENT LOCKING

The first element that we will look at is the shell element. For the mathematical development of the element, a one-dimensional model is used, but the premise is the same as in the full two-dimensional case. The element mode shapes will be presented in the one-dimensional case. The deflection solution was calculated by building the beam and solving the analysis in Excel.

3.1   Element Mode Shapes

The first step that we need to accomplish when building the element is to define the displacement field across the element. The displacement at each node must be completely independent of the other nodes in the element. This is done by creating a shape function that has a value of one at one node and zero at all the other nodes. These shape functions are added together in a linear combination with each shape function multiplied by the value at a particular node. The shape functions are written with respect of the local variable r and can be seen in Figure 6.

$$h_1 = \frac{1}{2}(r+1)$$

$$u(r) = h_1(r)u_1 + h_2(r)u_2$$
$$\phi(r) = h_1(r)\phi_1 + h_2(r)\phi_2$$

$$h_2 = -\frac{1}{2}(r-1)$$
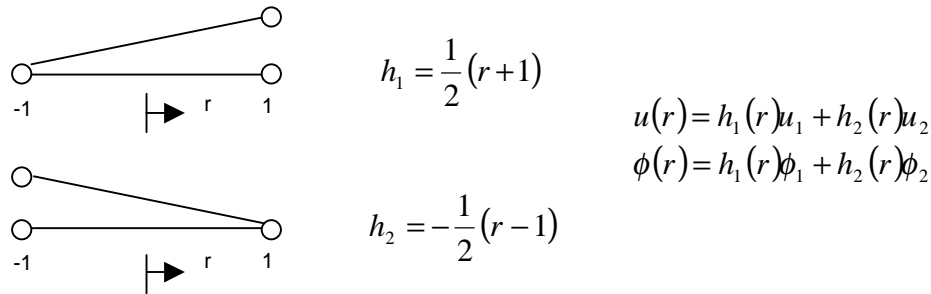
Figure 6. Shell Element Shape Functions.

The displacement field can also be written in matrix form. This will be a more advantageous form for later work.

$$\begin{vmatrix} u(r) \\ \phi(r) \end{vmatrix} = \begin{bmatrix} h_1 & 0 & \vdots & h_2 & 0 \\ 0 & h_1 & \vdots & 0 & h_2 \end{bmatrix} \begin{vmatrix} u_1 \\ \phi_1 \\ u_2 \\ \phi_2 \end{vmatrix}$$

$$\underline{u}(r) = H(r)\underline{\hat{u}}$$

The next step is to define the strain field in the element. There are two types of strain just as it was in the development of the exact solution. The bending strain and the shear strain are defined the same way as before.

$$K = \frac{d\phi}{dx} = \frac{d\phi}{dr}\frac{dr}{dx} = \frac{2}{l}\frac{d\phi}{dr}$$

$$\gamma = \frac{du}{dx} - \phi = \frac{du}{dr}\frac{dr}{dx} - \phi = \frac{2}{l}\frac{du}{dr} - \phi$$

The curvature and the shear deformation can also be expressed in matrix form. The B matrix is called the strain-interpolation matrix. In this notation, the prime marking indicates a derivative with respect to the local coordinate r, and l is the global element length.

$$\begin{vmatrix} K \\ \gamma \end{vmatrix} = \begin{bmatrix} 0 & \dfrac{2}{l}h_1' & 0 & \dfrac{2}{l}h_2' \\ \dfrac{2}{l}h_1' & -h_1 & \dfrac{2}{l}h_2' & -h_2 \end{bmatrix} \begin{vmatrix} u_1 \\ \phi_1 \\ u_2 \\ \phi_2 \end{vmatrix} \qquad \underline{\varepsilon}(r) = B(r)\underline{\hat{u}}$$

Expressing the our strain energy equation similarly to the exact solution form, and then converting it into matrix notation points out the form for the stiffness matrix described in the background portion of the introduction. J is the Jacobian matrix expressing the transformation from the local to the global coordinates. In this case there is only one transformation, which was earlier expressed as l/2.

$$V = \frac{1}{2}\int_{-1}^{1} EI\,(K)^2\,\frac{l}{2}\,dr + \frac{1}{2}\int_{-1}^{1} G\kappa\,(\gamma)^2\,\frac{l}{2}\,dr$$

$$V = \frac{1}{2}\int_{-1}^{1} \lfloor K \quad \gamma \rfloor \begin{bmatrix} EI & 0 \\ 0 & G\kappa \end{bmatrix} \begin{vmatrix} K \\ \gamma \end{vmatrix} \frac{l}{2}\,dr$$

$$V = \frac{1}{2}\underline{\hat{u}}^T \left[\int_{-1}^{1} B^T CB \, \|J\| dr \right] \underline{\hat{u}} = \frac{1}{2}\underline{\hat{u}}^T K \underline{\hat{u}}$$

The stiffness matrix is a way of expressing the relationship between an applied force at one position on a structure, and the response at some other position. The relationships are assumed to be linear, letting us use the follow form for the equilibrium position. Linearity also allows us to combine several elements together by adding the common matrix entries for common nodes.

$$K\underline{u} = \underline{F}$$

There are several interesting aspects to a structure's stiffness matrix. The mode shapes that an element or structure can assume and their frequencies can be found by extracting the eigenvalues and eigenvectors from the stiffness matrix. The eigenvectors describe the displacement of each node while the associated eigenvalue predicts the natural frequency for that mode.

The shell element has four modes, two rigid body modes and two elastic modes. The rigid body modes have a frequency of zero, while the elastic modes have non-zero frequency. The eigenvectors are shown with normalized values that make the magnitude of the vector one. It is important to also note that each mode is orthogonal to the others. Any normalized eigenvector multiplied by another is equal to zero, while any normalized eigenvalue squared is equal to one.

$$\phi_1 = \begin{vmatrix} \dfrac{1}{\sqrt{2}} \\ 0 \\ 1 \\ \dfrac{1}{\sqrt{2}} \\ 0 \end{vmatrix} \qquad \lambda_1 = 0$$

$$\phi_2 = \begin{vmatrix} \dfrac{5}{\sqrt{68}} \\ \dfrac{-3}{\sqrt{68}} \\ \dfrac{-5}{\sqrt{68}} \\ \dfrac{-3}{\sqrt{68}} \end{vmatrix} \qquad \lambda_2 = 0$$

$$\phi_4 = \begin{vmatrix} \dfrac{3}{\sqrt{68}} \\ \dfrac{5}{\sqrt{68}} \\ \dfrac{-3}{\sqrt{68}} \\ \dfrac{5}{\sqrt{68}} \end{vmatrix} \qquad \lambda_3 = 4.15\text{E}+6$$

$$\phi_3 = \begin{vmatrix} 0 \\ -\dfrac{1}{\sqrt{2}} \\ 0 \\ \dfrac{1}{\sqrt{2}} \end{vmatrix} \qquad \lambda_4 = 1.02\text{E}+6$$
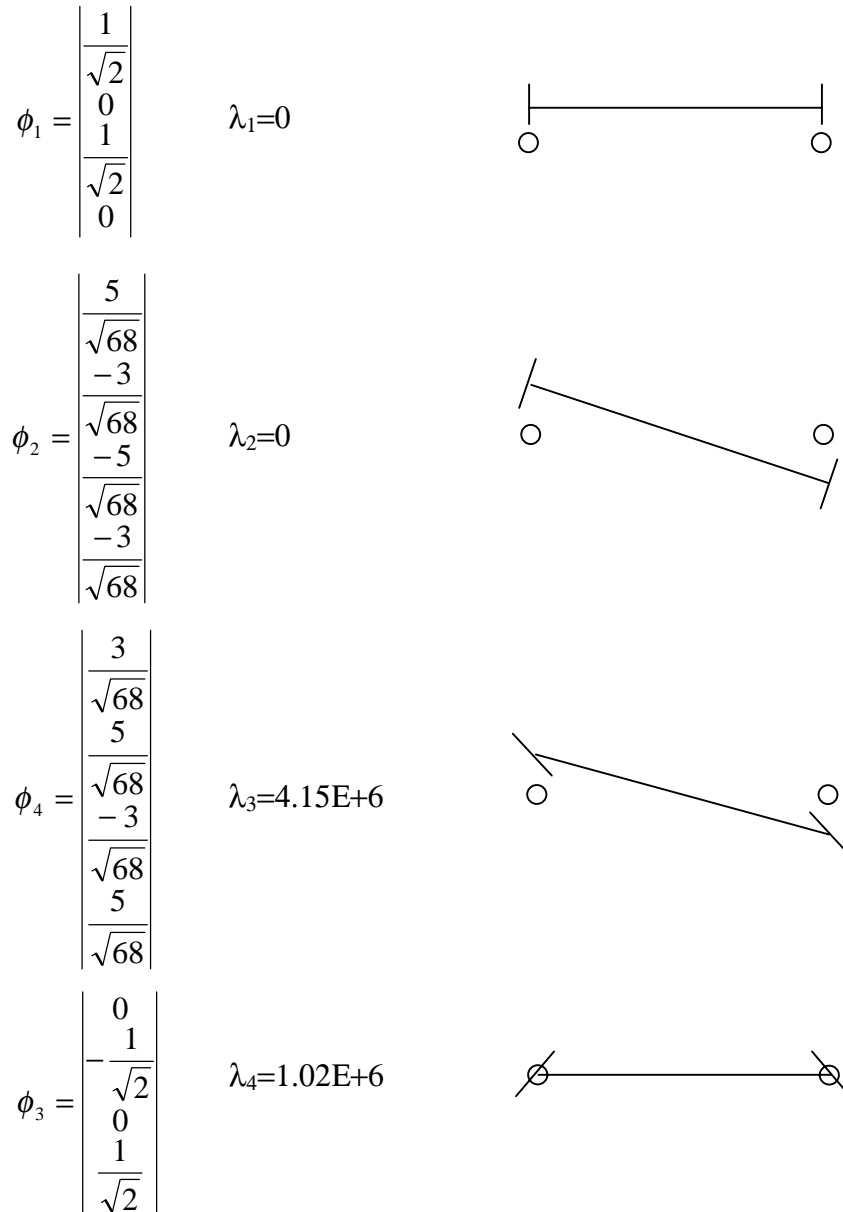
Figure 7. Shell Element Mode Shapes.

3.2   Deflection Solution

The final solution is a linear combination of the mode shapes; each multiplied by a modal participation factor. It is easier to solve the set of simultaneous linear equations than it is to find the modal participation factors. Most times the modal participation factors are extraneous to the final deflection and stress results.

Demonstrating the ease of using FEM technique on simple geometry, the system is solved for using Excel. The speed that the solution approaches the exact solution is dramatic. Unfortunately, because of the shear locking, it will not become apparent until changes are made to the integration scheme.

The meshing scheme used on the beam is to divide it equally along the length of the beam. Cases of one, two, and three elements are inspected.

Gaussian integration is used to evaluate the stiffness matrix. By sampling a limited number of places, you can evaluate a polynomial integral exactly the over a region. The number of sampling points is determined by the degree of the polynomial that you wish to evaluate. N sample points can exactly evaluate an integral of $(2n-1)$ order. The polynomial in the stiffness matrix is second order so there must be a minimum of two sample points. The points must be the zeroes of the Legendre Polynomial. For n equal two this means that the sample points will be $r=\pm 3^{-\square}$. There must also be a weighting factor multiplied by the results at each sample points. For n equal two, the weight factor happens to be one for both points. This yields the following as the integrated stiffness matrix for an element length of ten.

$$K = \begin{bmatrix} 183081 & 915404 & -183081 & 915404 \\ 915404 & 6103177 & -915404 & 3050863 \\ -183081 & -915404 & 183081 & -915404 \\ 915404 & 3050863 & -915404 & 6103177 \end{bmatrix}$$

The first two degrees of freedom are constrained to zero displacement. This means when solving for the equilibrium solution it is only necessary to solve for the last two degrees of freedom. The applied load is a point force on the unconstrained node. That makes our final system of equations the following. The same is done for the two and three element systems. The difference being

$$\begin{vmatrix} u_2 \\ \phi_2 \end{vmatrix} = \begin{bmatrix} 183081 & -915404 \\ -915404 & 6103177 \end{bmatrix}^{-1} \begin{vmatrix} 100 \\ 0 \end{vmatrix}$$

the common degrees of freedom are added together creating a banded stiffness matrix. The displacements are shown in the following chart compared to the exact displacements.
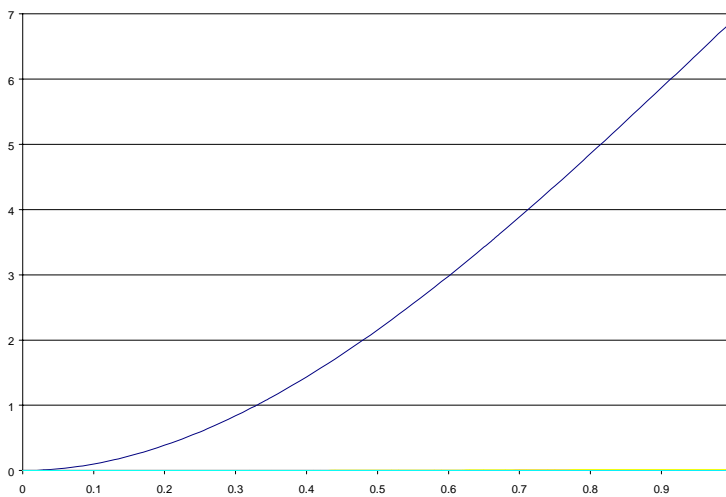
Number of Elements	Tip Displ.
Exact	6.897098
One Element	0.002184
Two Elements	0.008729
Three Elements	0.019609

Figure 8. Locked Beam Displacements.

It is obvious from either Figure 7, or the table of tip displacements that the locking phenomenon is a severe flaw in the method. It is clear something is very wrong in this simple case, but in complex loading of a shell modeled blade it would not be as easy to determine that the shear deformation is not contributing.

3.3   Cause of Locking

An over-constrained system, or perhaps better put, an overly inflexible set of shape functions, causes shears locking. Two linear functions only have four unknowns to determine. After applying the four boundary conditions there are no more unknowns to manipulate. This means that the chances that the shape functions will satisfy the differential equations are slim. It is easy to see this through working the example we have been working.

$$\frac{u}{L}(\eta)=c_1\eta+c_2 \qquad\qquad \phi(\eta)=c_3\eta+c_4$$
$$\frac{u'}{L}(\eta)=c_1 \qquad\qquad\qquad \phi'(\eta)=c_3$$

The finite element code does not apply all the boundary conditions and then try to satisfy the differential equations. It applies the geometric boundary conditions, then lets the natural boundary conditions come through the minimization process. Following this procedure, we start by applying the geometric boundary conditions.

$$\phi'\big|_{\eta=1}=0=c_3 \qquad\qquad \frac{u}{L}\bigg|_{\eta=0}=0=c_2$$
$$\phi(\eta)=c_4\eta \qquad\qquad\qquad \frac{u}{L}(\eta)=c_1\eta$$

Next, the differential equations are satisfied. This produces the locking results.

$$\phi'-\frac{u''}{L}=0 \qquad\qquad k\phi-\phi''-k\frac{u'}{L}=0$$
$$c_3-0=0\Rightarrow c_3=0 \qquad 0-0-kc_1=0\Rightarrow c_1=0$$
$$\phi(\eta)=0 \qquad\qquad\qquad \frac{u}{L}(\eta)=0$$

The actual results are not zero displacement because the minimization process tries to impose the natural boundary conditions while solving the differential equations. This would enforce some tip displacement, but it can be shown that the tip displacement approaches zero as the aspect ratio of the element increases.

3.4   Element Applicability

Most commercial packages do not use the type of integration scheme on shell elements because of the severe problems shown above. One notable exception is when analyzing pressure vessels. Some codes use the fact that the fully integrated shell element does not react to bending loads to better model the

steady state equilibrium of pressure vessels. The elements will only deform axially, so surfaces will remain perpendicular to the pressure.

Otherwise codes will automatically use reduced integration. It will be shown later that reduced integration is an easy solution to the shear-locking problem. Reduced integration causes some other problems of which the user must be aware.

The constitutive law and strain displace relationships will enforce equilibrium within the element even if flawed boundary conditions provide the incorrect forces. The finite element method does not enforce equilibrium between the elements. That is why an increasing number of elements creates a better solution. It should be noted that it is not the correctness of the FEM that causes a finer mesh to be more exact *in this case*, but the flaw in the method that does.
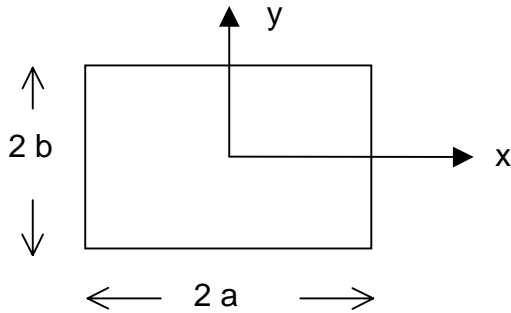
SECTION 4
BRICK ELEMENT LOCKING

Like the shell element development, the brick element will also be pursued one dimension lower than the actual element. The brick element will be shown as a two dimensional element like a membrane element. This reduces the elemental stiffness matrix size from 24x24 to 8x8. The modes shapes are calculated on Maple, while the deflection solution was found using Nastran.

4.1   Potential Energy

The potential energy equation is very different from the ones used before. This is because the dimension of depth is added, eliminating the need to add redundant degrees of freedom for rotation. The potential energy is defined by the Cauchy formulation of strain energy. Strain energy is likened to work done on the material that will be recovered when the load is removed.

$$V = \int_{-b}^{b}\int_{-a}^{a} \underline{\varepsilon}^{T}\underline{\sigma}\,dxdy$$

$$\underline{\varepsilon} = \begin{vmatrix} \varepsilon_1 \\ \varepsilon_2 \\ \gamma_{12} \end{vmatrix} \qquad \underline{\sigma} = \begin{vmatrix} \sigma_{11} \\ \sigma_{22} \\ \tau_{12} \end{vmatrix}$$

Figure 9. Brick Element Dimensions

4.2   Element Mode Shapes

Again, the mode shapes start with the shape functions for the element. The local coordinates used to define the shape functions extend from negative one to one in each direction. The nodal numbering is defined starting from the first quadrant increasing by the right-hand rule.
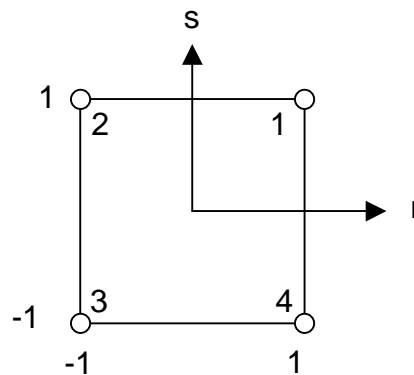
Figure 10. Brick Element Local Coordinates.

The shape functions have a unit value at the node of interest, and zero values at all other nodes. A typical shape function is shown after the shape functions below.

$$h_1 = \frac{1}{4}(1+r)(1+s) \qquad\qquad h_3 = \frac{1}{4}(1-r)(1-s)$$

$$h_2 = \frac{1}{4}(1-r)(1+s) \qquad\qquad h_4 = \frac{1}{4}(1+r)(1-s)$$

Figure 11. Brick Element Shape Function.

The next step is to define the strain-displacement relationship. The differences from the shell element are axial strain in two dimensions and that the shear str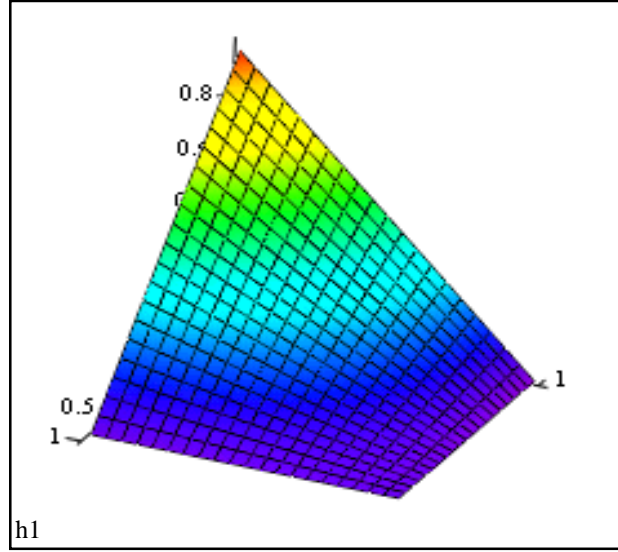ain is defined differently. The k index in the matrix notation is to denote the shape function number. The strain interpolation matrix will be a three by eight matrix in this example.

$$\varepsilon_1 = \frac{du}{dx} = \frac{du}{dr}\frac{dr}{dx}$$

$$\varepsilon_2 = \frac{dv}{dy} = \frac{dv}{ds}\frac{ds}{dy}$$

$$\gamma_{12} = \frac{du}{dy} + \frac{dv}{dx} = \frac{du}{ds}\frac{ds}{dy} + \frac{dv}{dr}\frac{dr}{dx}$$

$$\begin{vmatrix} \varepsilon_1 \\ \varepsilon_2 \\ \gamma_{12} \end{vmatrix} = \Lambda \begin{bmatrix} \frac{1}{a}h_{k,r} & 0 \\ 0 & \frac{1}{b}h_{k,s} \\ \frac{1}{b}h_{k,s} & \frac{1}{a}h_{k,r} \end{bmatrix} \Lambda \, \hat{\underline{u}}$$

The final ingredients needed to find the stiffness matrix, and then the mode shapes, are the constitutive laws. The plane stress relationships are used to define the connection between the strain and the stress.

$$\begin{vmatrix} \sigma_{11} \\ \sigma_{22} \\ \tau_{12} \end{vmatrix} = \frac{E}{1-v^2} \begin{bmatrix} 1 & v & 0 \\ v & 1 & 0 \\ 0 & 0 & \frac{1-v}{2} \end{bmatrix} \begin{vmatrix} \varepsilon_1 \\ \varepsilon_2 \\ \gamma_{12} \end{vmatrix}$$

4-2

The Jacobian becomes a more complex matrix because of the second dimension added to the problem. The Jacobian is defined in the following manner. The Jacobian is used to transform the coordinates from the global to the elemental coordinates.

$$\begin{vmatrix} dx \\ dy \end{vmatrix} = \begin{bmatrix} \dfrac{dx}{dr} & \dfrac{dx}{ds} \\ \dfrac{dy}{dr} & \dfrac{dy}{ds} \end{bmatrix} \begin{vmatrix} dr \\ ds \end{vmatrix}$$

$$\begin{vmatrix} dx \\ dy \end{vmatrix} = J \begin{vmatrix} dr \\ ds \end{vmatrix}$$
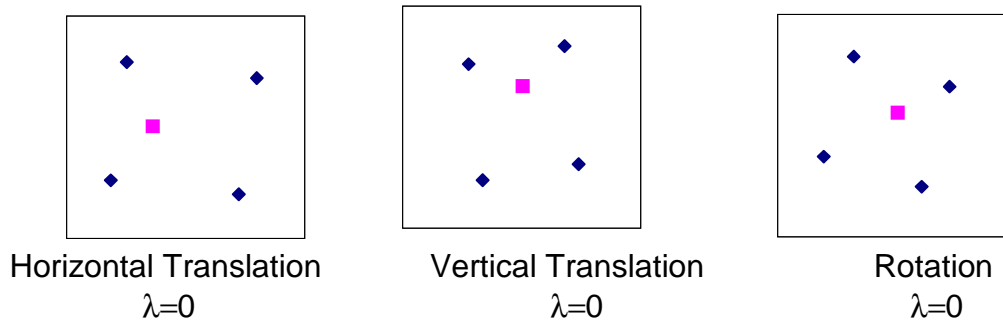
Combining all the relationships into the strain energy equation will produce the stiffness matrix, just as it did for the shell element. The same notation applies as before. The B matrix is the strain interpolation matrix. The matrix used in the constitutive law is the C matrix.

$$V = \frac{1}{2} \int_{-b}^{b} \int_{-a}^{a} \left(\underline{\varepsilon}^T \underline{\sigma} \right) dxdy$$

$$V = \frac{1}{2} \int_{-b}^{b} \int_{-a}^{a} \left(\underline{\hat{u}}^T B^T C B \underline{\hat{u}} \right) dxdy$$

$$V = \frac{1}{2} \underline{\hat{u}}^T \left(\int_{-1}^{1} \int_{-1}^{1} B^T C B \left| J \right| drds \right) \underline{\hat{u}} = \underline{\hat{u}}^T K \underline{\hat{u}}$$

The stiffness matrix for this element is an eight by eight matrix. This means there will be eight mode shapes. There are three rigid body modes, two translations and one rotation. There are five elastic modes, one uniform, two shear, and two bending modes. All of the modes are shown below with the associated eigenvalue. The rigid body modes have a zero eigenvalue, meaning that they all must be constrained or the stiffness matrix will be singular.

Horizontal Translation
$\lambda=0$

Vertical Translation
$\lambda=0$

Rotation
$\lambda=0$

Figure 12. Brick Element Rigid Body Modes.

Bending
λ=0.4976

Bending
λ=0.4976

Uniform Contraction
λ=1.47

Uniaxial
λ=0.7575

Shear
λ=0.7575
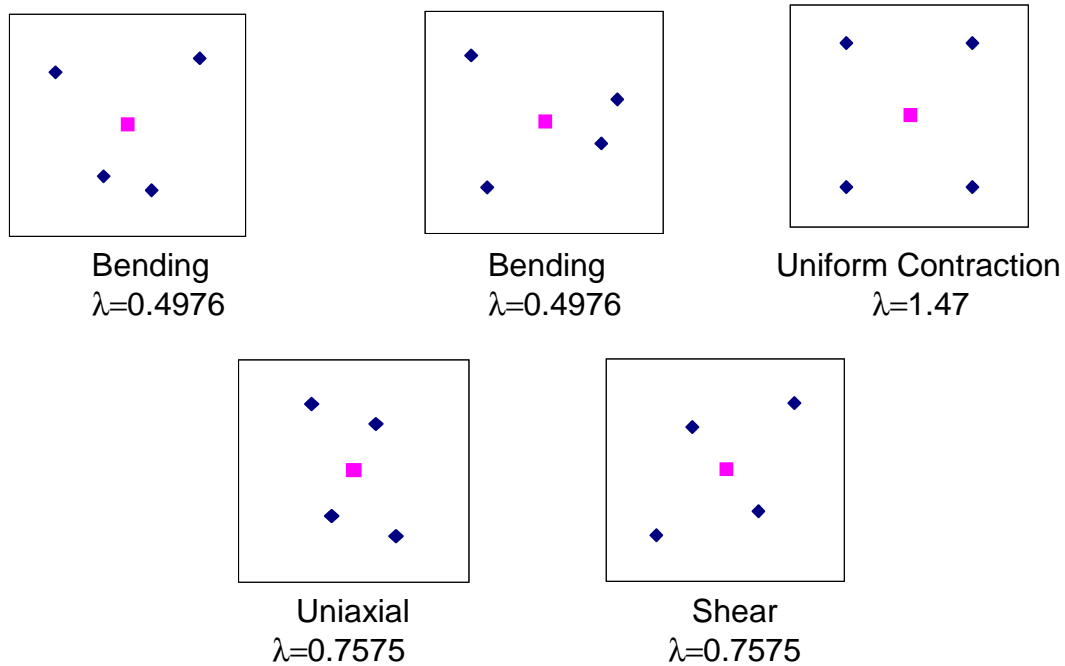
Figure 13. Brick Element Bending Modes.

4.3   Deflection Solution

Patran generated the code to analyze the deflection solution in Nastran. There were two models used. The first model had 180 elements, each with eight nodes. The elements each had a length and width of a third and were one-tenth inch deep. This model is shown in Figure 14. The other model had the same dimensions, but the elements were one-fifth inch long and wide.

0.1

0.333   0.333

30 elements
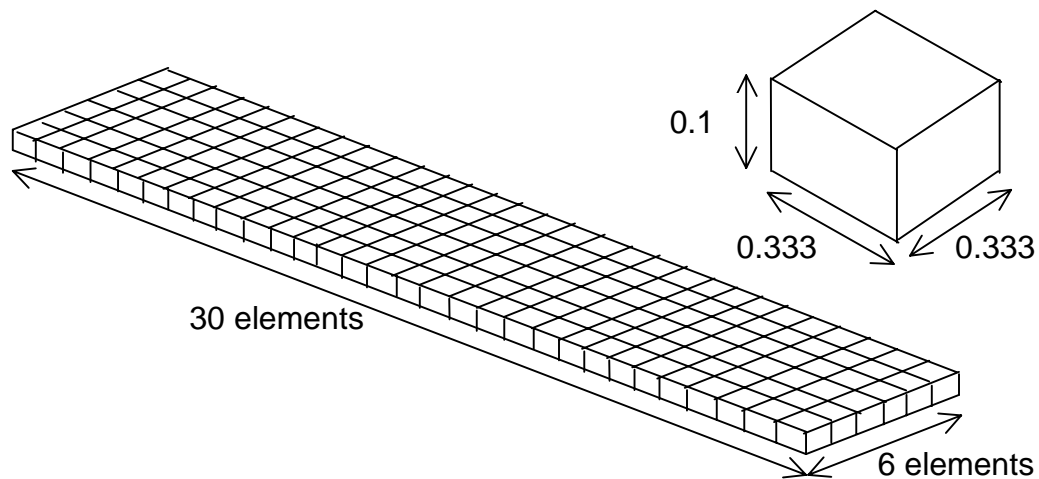
6 elements

Figure 14. Brick Element Beam Model.

Both beams are held to the same boundary conditions. At one end of the beam the end nodes were set to zero displacement out of the plane. The center two

nodes were additionally held to no displacement within the plane either. The other end had a 100-pound downward force applied to the upper center node.

There are several different integration methods that can be used by Nastran to evaluate the stiffness matrix. The option used in this model told Nastran to use full integration to evaluate the stiffness matrix. This meant for two gauss points to be used in each direction in obtaining the exact solution since one linear equation multiplied by another creates a quadratic equation. As in the shell element, full integration under shear loading creates locking.
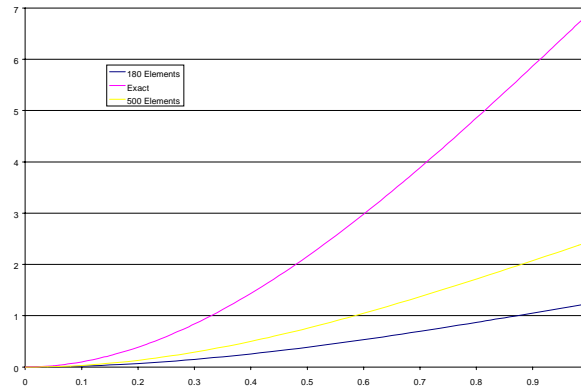

Figure 15. Locked Brick Element Deflection Solution.

Even with fifty elements along the span of the beam, the deflection is only about one-third of what the exact solution is. This shows that although the model will still converge to the correct solution through the discontinuity of equilibrium, the efficiency of the method is dramatically reduced.

4.4   Natural Frequencies

Using the same integration scheme, but using a modal analysis instead of a linear analysis, Nastran will give the first ten modes and their associated frequencies. These are compared to the calculated values in the table below.

	FEM	Calculations	Error
1 lateral	188.48	194.52	-3.11%
1 torsion	99.24	89.66	10.69%
2 torsion	311.76	268.97	15.91%
3 torsion	563.24	448.28	25.64%
4 torsion	872.36	627.60	39.00%
1 bend	16.34	9.73	67.97%
2 bend	102.29	60.95	67.82%
3 bend	285.75	170.67	67.43%
4 bend	559.20	334.44	67.21%
5 bend	922.83	552.85	66.92%

The locking effect's dependence on the aspect ratio of the element and the structure is clear. In the lateral deflection, the structural length (10) divided depth (2) is five, while in the bending direction, the quotient (10/0.1) is 100. The error is

approximately twenty times greater as is the quotient. Further, the element has an aspect ratio of over three to one for the bending mode and just one to one for the lateral bending.

The percent error is also dependent on the mode shape number. Some modes have different amounts of curvature in each direction. The more curvature that is required, the more error there will be in general. The bending modes are all similar in error, potentially because it is the maximum error limit.

4.5   Cause of Locking

The element locks because it is an inflexible system just as the shell element is. The definition of linear is a little different in these shape functions, creating a more flexible system, but even this added flexibility is not enough to unlock the system. The existence of four nodes implies that we will need four coefficients to correctly determine the system. Unfortunately, two linear functions of independent variables only have three coefficients when combined since the constants can be added together. This is how a non-linear term gets added into the linear shape functions shown below.

$$u(x, y) = c_1 x + c_2 y + c_3 xy + c_4$$
$$v(x, y) = c_5 x + c_6 y + c_7 xy + c_8$$

Just as in the example with the shell element the brick element is subject to both geometric and natural boundary conditions. Each displacement field has one of each type at both ends of the element. Take as an example the element with the coordinate axes shifted to the position shown below to make the equations more easily examined. The single equation requiring no displacement in the u direction acts as two separate constraints at x=0.
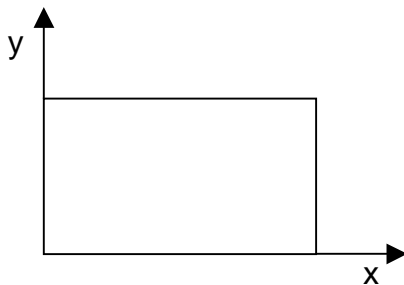
$$u(0, y) = c_2 y + c_4 = 0$$
$$v(0, y) = c_6 y + c_8 = 0$$

but because the equation must hold for all values of y the only solution is:

$$c_2 = 0 \qquad c_4 = 0$$
$$c_6 = 0 \qquad c_8 = 0$$

Figure 16. Brick Element with Shifted Axes.

Likewise, the boundary conditions on the other end relating deflection to the applied shear also add four constraints. These eight constraints combined with two differential equations create a total of ten constraints and only eight unknowns. The system is over-constrained and tends toward the trivial solution trying to satisfy all conditions.

SECTION 5
SHELL ELEMENTS WITH REDUCED INTEGRATION

Locking needs to be removed in order to predict the stress correctly and displacement fields in some structures. There must be changes made to the element to have it work correctly. There are two main ways to this: change the degrees of freedom to match the number of constraints or modify how the stiffness matrix is built so that the constraints can be followed with the same number of degrees of freedom.

The number of degrees of freedom is dependent on the number of nodes. By introducing a node at the mid-span point of the element, two additional degrees of freedom are introduced. This brings the total to three translations and three rotations, equaling the constraints. There is no locking in this new element. This is similar to the method followed in the brick element with a bubble mode. Changing the shape functions to a higher order polynomial increases the number of constants that must be solved for to at least equal to the number of constraints.

We will leave that for the next section and now see what can be done if there is a need to use a two-node element instead of the one with three nodes. If the stiffness matrix is determined by using a lower order Gaussian integration the element will no longer have locking. This section will focus on this reduced order integration technique.

5.1   Mode Shapes

The shape functions will still be linear for this analysis. This makes the function to be integrated a second order polynomial when the shape functions are multiplied together. To exactly evaluate a second order polynomial would require two Gauss points. For this analysis we only use one Gauss point.

This changes the values of the stiffness matrix and therefore possibly the eigenvalues and eigenvectors. The overall eigenvectors do not change, but an eigenvalue does change. The bending mode has an eigenvalue that was lowered by three orders of magnitudes. This means that the amount of energy that is needed to cause a change in the deflection is much less than the locking situation, allowing the locked configuration to unlock.

The reduced order integration will exactly integrate the equations in the stiffness matrix, except for those in the second or fourth column and the second or fourth row. That is because when the strain interpolation matrix is transposed and multiplied by itself, only those positions have a term of r squared. This is apparent when we recall the strain interpolation matrix that was developed before is as shown below.

$$\begin{vmatrix} K \\ \gamma \end{vmatrix} = \begin{bmatrix} 0 & \dfrac{-1}{l} & \vdots & 0 & \dfrac{1}{l} \\ \dfrac{-1}{l} & \dfrac{1}{2}(r-1) & \vdots & \dfrac{1}{l} & -\dfrac{1}{2}(r+1) \end{bmatrix} \begin{Vmatrix} u_1 \\ \phi_1 \\ u_2 \\ \phi_2 \end{Vmatrix} \qquad \underline{\varepsilon}(r) = B(r)\underline{\hat{u}}$$

The only mode shape that is completely defined by the stiffness in the rotations is the fourth mode. It is also the only mode that changes eigenvalues. All other eigenvalues are based on the stiffness of either, combined rotation and translation (odd column and even row and vice versa), or pure translation (odd rows and columns).

5.2 Force-Displacement Matrix

The construction of the stiffness matrix through full integration of the constitutive equations and the strain displacement relationship effectively minimizes the unknown constants in the deflection solution in a given ratio in accordance with the governing laws. The matrix inversion and the applied forces then solve for the magnitude of that ratio by creating a linear combination of those deflection ratios. This is obvious when you view the equation.

$$d = K^{-1}F$$

0.001912	0.001147	0.005732	0.001147	0.009552	0.001147
0.001147	0.000689	0.003441	0.000689	0.005736	0.000689
0.005732	0.003441	0.019103	0.004589	0.034383	0.004589
0.001147	0.000689	0.004589	0.001378	0.009177	0.001378
0.009552	0.005736	0.034383	0.009177	0.066854	0.010324
0.001147	0.000689	0.004589	0.001378	0.010324	0.002067

$= K^{-1}$

The inverse of the stiffness matrix is clearly a way to combine the individual shape functions. To represent this, the figure below shows the deflection for a unit force applied at a particular node. The final solution is a linear combination of each of these shapes, each with the participation coefficient equal to the load applied at the respective node.
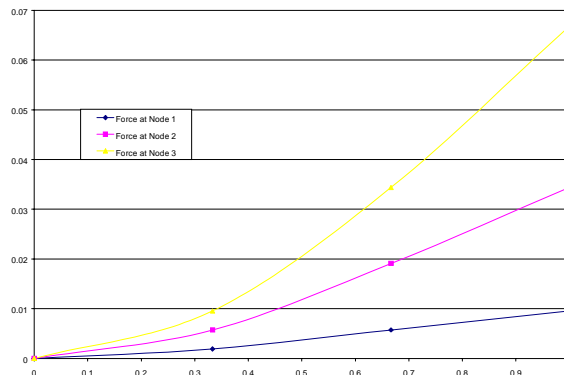
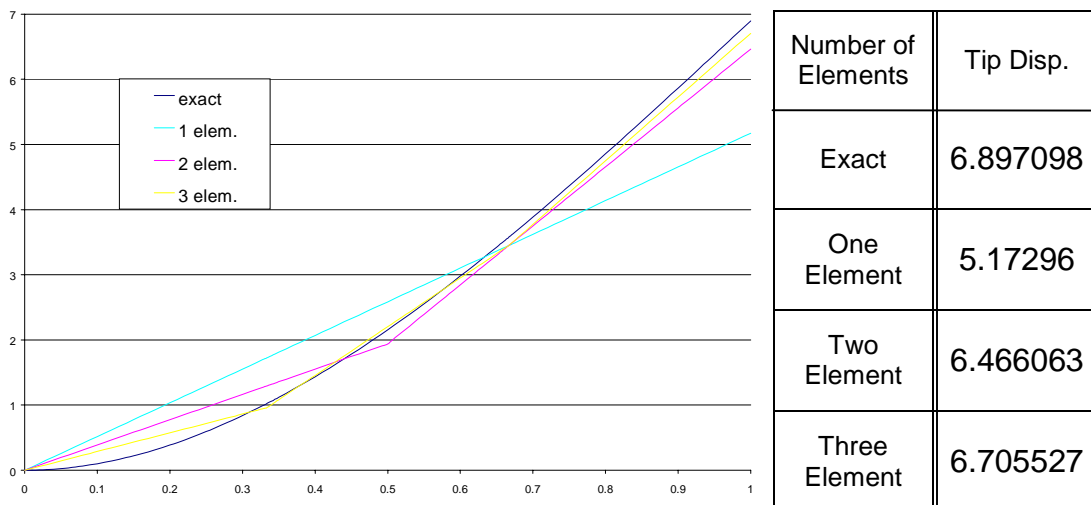**Figure 17. Beam Deflection Mode Shapes.**

The first thing that can be seen is that the unit force creates a greater displacement when applied at a more outboard node. This makes sense because it would create a greater moment about the beam root.

The inverted stiffness matrix also shows that the strain-displacement relationships are enforced. This is best seen in the first column representing a load applied at the first node. The rotation at all further nodes are equal to the rotation at the first node. This is because the beam's curvature is proportional to the moment at that point. Outboard of the applied force there is no reaction force, nor reaction moment. This means that curvature outboard should be zero implying a constant rotation and slope. Both of these implications are found to be true in the graph above.

5.3   Deflection Solution

The difference that this makes in the final solution is drastic. The effect of making the change in rotation easier makes the solution converge towards the exact solution very quickly.

Once again the solution was done on Excel. The stiffness matrix was inverted by using the row-echelon format. The inverted matrix multiplied by the force vector will produce the deflection solution. The solution is found for one, two, and three elements across the length of the beam. Solutions are compared both in the graph and in the table of tip displacements.

Number of Elements	Tip Disp.
Exact	6.897098
One Element	5.17296
Two Element	6.466063
Three Element	6.705527

Figure 18. Reduced Integration Shell Deflection Solution.

The elements are more accurate as the actual deflection approaches a linear function. When there is more curvature in the solution the elements must be smaller to stay close to the exact answer. Even so, the error is small considering there are only three elements. In fact, the solution converges to the exact solution very quickly. Remember that the locked solution yields a zero deflection solution for high aspect ratio elements such as these.

The effect the change has on the rotation is more curious. The reduced energy to cause rotation allows the tip rotation to equal the exact for any number of elements, including only one. Therefore the stiffness matrix applies the tip moment boundary condition exactly.

5.4   Natural Frequencies

To find the first ten natural frequencies of the system there must be at least ten degrees of freedom. This means that you would need to invert at least a ten by ten matrix, more if you wish to have more accuracy. This makes the reverse echelon method impractical. Instead, Nastran solved the system of equations.

For this example a system of 80 four-node shell elements predicted the frequencies. The beam had four elements across the width and twenty along the length. A figure showing the mesh is located below.
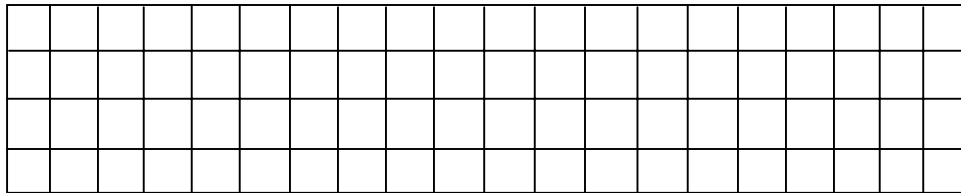
Figure 19. Meshing of Reduced Order Shell Elements.

The higher number of elements attempts to keep the curvature close to zero across any given element. This will reduce the error in energy in a given mode and make the frequency closer to the exact frequency. The improvement of the frequency prediction over the locked brick elements is apparent. These could be improved by adding more elements. They would be best added across the width to rectify the error in the torsion modes.

	FEM	Calculations	Error
1 lateral	188.42	194.52	-3.14%
1 torsion	90.79	89.66	1.26%
2 torsion	276.92	268.97	2.96%
3 torsion	476.23	448.28	6.23%
4 torsion	696.26	627.60	10.94%
1 bend	9.85	9.73	1.23%
2 bend	61.50	60.95	0.90%
3 bend	172.12	170.67	0.85%
4 bend	337.46	334.44	0.90%
5 bend	557.91	552.85	0.98%

The higher order torsion modes have the most error because they have components of curvature in both the length and width directions. The higher the mode the more nonlinear the deflection is across a given element, causing the error to increase as the modal number increases.

5.5 Element Applicability and Meshing Criteria

This element is a good one to use in most situations. It is the only integration technique used by most codes for shell elements. The major limitation to the reduced integration techniques is that it cannot be used when the stiffness or mass matrix is not symmetric. So, if there is an active control system or energy losses not associated with damping forces the reduced integration technique will not work.

The best method of meshing is to have as many elements as possible across the stress gradient, the steeper the stress gradient the more elements required. In our example the stress gradient lines run across the width of the beam. This implies that for best results single elements could run across the width of the beam, giving the most possible elements across the stress flow.

In most cases the stress gradient is not known before the analysis. The best idea is to then keep the elements close to an aspect ratio of one to get an initial mesh. After the general stress field is known a refined mesh can be created.

There will always be a tradeoff between the increase in accuracy and the increase in computational costs. The increase of computational time is rough proportional to the number of elements squared. Ultimately the solution to this tradeoff is left to the analyst.

SECTION 6
BRICK ELEMENT WITH BUBBLE NODE

The same concepts that could be applied to the shell element to relieve the locking can be applied to the brick element. Either the element can be given more degrees of freedom or the stiffness matrix can be evaluated a different way.

This section will look at how the addition of an additional node, not on the boundary with another element, can add the needed flexibility to unlock the system. The node will be placed at the center of the element in the two dimensional model of the full brick element. The additional node, with its associated degrees of freedom, will bring the total degrees of freedom equal to the total number of constraints.

6.1 Shape Functions and Mode Shapes

There will be changes to the mode shapes because of the introduction of the additional node. This new shape function should have a value of one at the origin and zero values on the edges. Additionally, the original shape functions must be changed as well. They all had a value of one quarter at the origin, whereas they should now have a value of zero. This is accomplished by subtracting a quarter of the new shape function from each of the old ones. The shape functions are shown here.
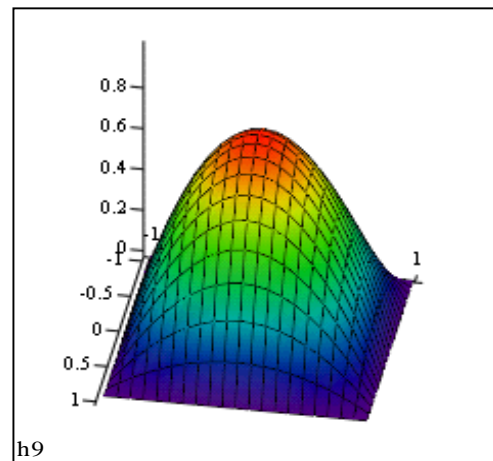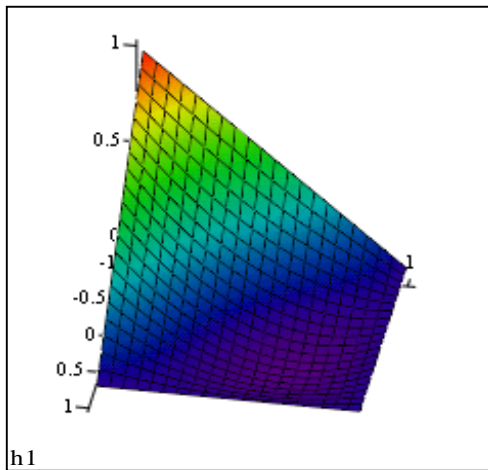
$$h_1 = \frac{1}{4}(1+r)(1+s) - \frac{1}{4}(1-r^2)(1-s^2) \qquad h_3 = \frac{1}{4}(1-r)(1-s) - \frac{1}{4}(1-r^2)(1-s^2)$$

$$h_2 = \frac{1}{4}(1-r)(1+s) - \frac{1}{4}(1-r^2)(1-s^2) \qquad h_4 = \frac{1}{4}(1+r)(1-s) - \frac{1}{4}(1-r^2)(1-s^2)$$
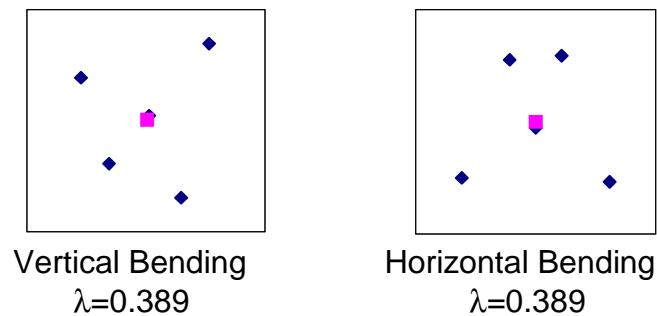
$$h_5 = (1-r^2)(1-s^2)$$

Figure 20. Brick Shape Functions Including the Bubble Modes.

The new shape function will increase the size of the stiffness matrix to a ten by ten matrix. This means that there are now ten eigenvalues and ten eigenvectors. The original eight are the same, but the two new ones are associated with the bubble node. These are called bubble modes because they are primarily a displacement of the bubble node without much deflection in the other modes.

The mode shapes remain the same for the stiffness matrix including the bubble node. The only change beside the addition of the bubble modes is the lowering of the bending modes' eigenvalue. This is evidence that the bending stiffness of this element is reduced. The modes and their eigenvalues are displayed in the figures below.

| Shearing | Uniaxial Tension | Biaxial Tension |
| $\lambda=0.7575$ | $\lambda=0.7575$ | $\lambda=1.47$ |
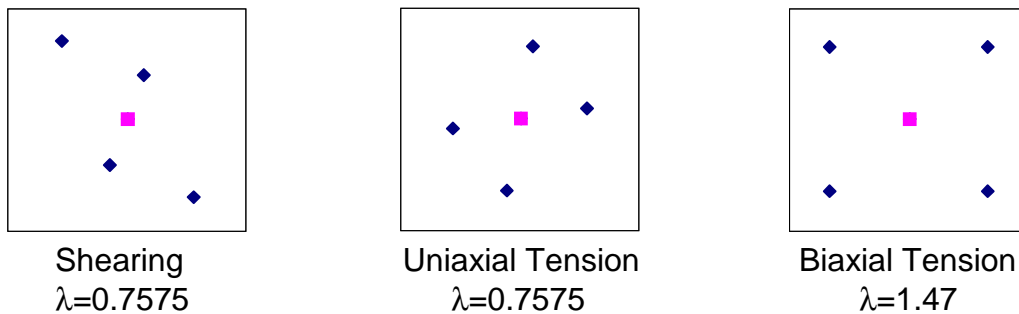
Figure 21. Brick Element Constant Strain Modes.

| Vertical Bending | Horizontal Bending |
| $\lambda=0.389$ | $\lambda=0.389$ |

Figure 22. Brick Element Bending Modes.

| Vertical Bubble Mode | Horizontal Bubble Mode |
| $\lambda=5.4165$ | $\lambda=5.4165$ |
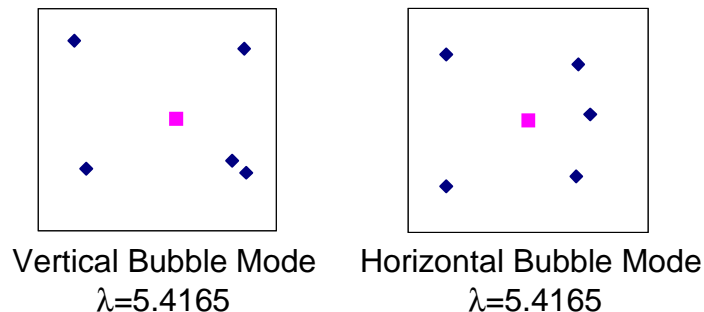
Figure 23. Brick Element Bubble Modes.

| Rotation | Horizontal Translation | Vertical Translation |
| $\lambda=0$ | $\lambda=0$ | $\lambda=0$ |
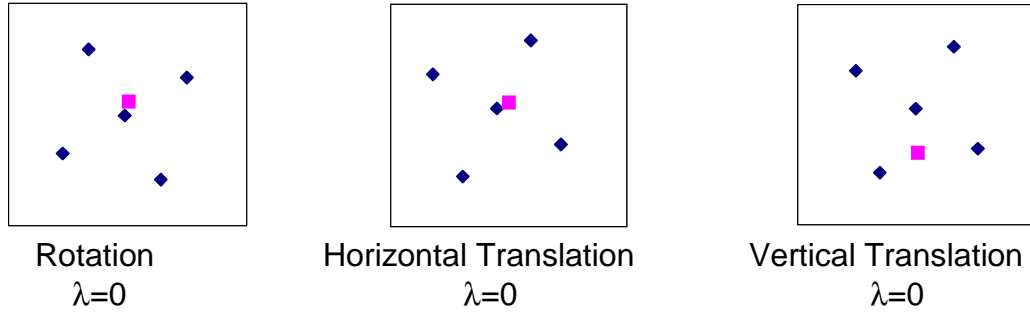
Figure 24. Brick Element Rigid Body Modes.

6.2   Solution Technique

The solution starts with assuming a shape function of the solution. The solution is quadratic in the horizontal and the vertical coordinates, as well as their combination. The new shape functions are shown below. Notice how there is a quartic polynomial term. It is included in the same manner that the quadratic term was included in the original brick development.

$$u = c_1 + c_2 x + c_3 y + c_4 xy + c_5 x^2 + c_6 y^2 + c_7 x^2 y + c_8 xy^2 + c_9 x^2 y^2$$

$$v = c_{10} + c_{11} x + c_{12} y + c_{13} xy + c_{14} x^2 + c_{15} y^2 + c_{16} x^2 y + c_{17} xy^2 + c_{18} x^2 y^2$$

These new shape functions are associated with eighteen unknown constants. In the same manner as explained in the section on why the brick elements lock, the two boundary conditions each impose three constraints on each of the new shape functions. Excluding the two differential equations, there are twelve constraints. This leaves six constants to be solved for by the differential equations. The equations might not be solved for exactly, but the answer can be much more accurate than when there was only one degree of freedom that could be solved for in the two differential equations.
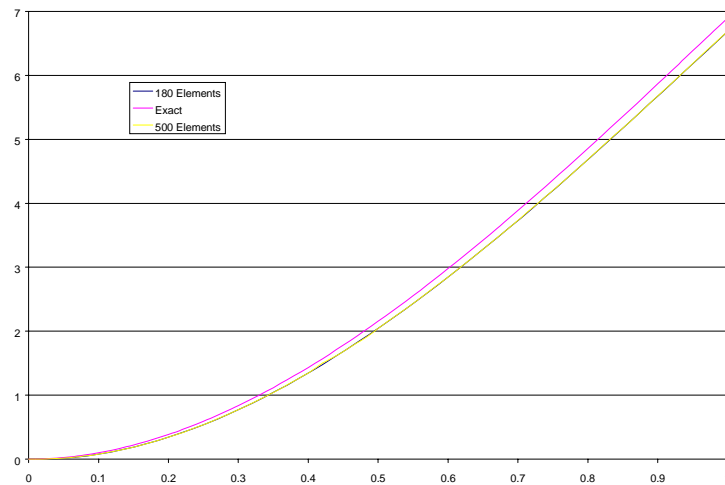
Figure 25. Bubble Mode Element Deflection.

The integration of the stiffness matrix during its formulation minimizes the error over the examined structure. This produces a deformed position that most accurately enforces all the boundary conditions as well as the differential equations. The linear static solution with the mesh described using fully integrated bubble modes shows a tip deflection of 6.73865. This is within 2.3% of the theoretical solution, a vast improvement over the elements without the bubble mode.

6.3   Matrix Inversion

A difficult part of solving a linear set of equations is that there can be n unknowns in n equations, where n can be very large. To solve for any particular variable, it is necessary to have one equation and one unknown. Two common ways of accomplishing this is to invert the matrix, thereby lumping all unknowns into one large unknown, and substituting equations which require a symbolic processor, but do yield a series of one unknown equations.

A good representation of the second part of the substitution method is shown in the following equations. Each equation only uses the values of the preceding equations plus an additional unknown. The first two equations solved for the unknowns are shown as well. The pattern is evident and easily repeatable.

$$\begin{bmatrix} L_{11} & 0 & 0 \\ L_{21} & L_{22} & 0 \\ L_{31} & L_{32} & L_{33} \end{bmatrix} \begin{vmatrix} x_1 \\ x_2 \\ x_3 \end{vmatrix} = \begin{vmatrix} c_1 \\ c_2 \\ c_3 \end{vmatrix} \qquad \begin{aligned} x_1 &= \frac{c_1}{L_{11}} \\[2mm] x_2 &= \frac{1}{L_{22}}\left(c_2 - L_{21}\frac{c_1}{L_{11}} \right) \end{aligned}$$

Finite element packages use this process to solve systems of equations because they are much faster than computing the inverse of a large matrix. Unfortunately, they must solve a system that is not of the form of a lower triangular matrix. There is a way to represent any square matrix as two triangular matrices and a diagonal matrix, and a symmetric matrix as a triangular matrix and a diagonal matrix. This method is shown in the equations below.

$$K = \begin{bmatrix} D_1 & K_{12} & K_{13} \\ K_{12} & D_2 & K_{23} \\ K_{13} & K_{23} & D_3 \end{bmatrix} = LDL^T$$

$$L = \begin{bmatrix} 1 & 0 & 0 \\ \dfrac{K_{12}}{D_1} & 1 & 0 \\ \dfrac{K_{13}}{D_1} & \dfrac{K_{23}}{D_2} & 1 \end{bmatrix} \qquad D = \begin{bmatrix} D_1 & 0 & 0 \\ 0 & D_2 & 0 \\ 0 & 0 & D_3 \end{bmatrix}$$

Now a single fully populated linear matrix equation can be solved by three simple linear equations.

$$K\underline{u} = \underline{F}$$

$$LDL^T\underline{u} = \underline{F} \qquad \textit{substituting} \qquad \underline{y} = DL^T\underline{u}$$

$$L\underline{y} = \underline{F}$$

$$DL^T\underline{u} = \underline{y} \qquad \textit{substituting} \qquad \underline{x} = L^T\underline{u}$$

$$D\underline{x} = \underline{y}$$

$$L^T\underline{u} = \underline{x} \qquad \textit{solve for unknown vector}$$

This might seem more complicated because three systems of equations must be solved instead of a single system, but they are much easier systems to solve. They also have an added benefit when dealing with a highly banded matrix as found in finite element applications. None of the matrices lose their bandedness, unlike the inverse of a banded matrix. The inverse of a banded matrix is normally a fully populated matrix which would take too much memory to perform calculations on it. For example, a ten thousand-degree of freedom system would have to have 100 megabytes of memory simply to hold the matrix in memory, let alone perform operations on it. The simple beam model shown above with 180 elements had 1260 degrees of freedom and would have needed about 1.6 megabytes of memory to hold the inverted matrix.

6.4   Natural Frequencies

The following model determined the natural frequencies of the system using Patran. It is the same 180-element model described above comprised of Hex8 brick elements.

**Figure 26. Patran Model Used to Determine Natural Frequencies.**

The following table shows the frequencies determined by the finite element analysis. The accuracy is very good in the bending modes but falls off in the torsion modes. Partly this is because of the higher strain energy in those modes. That can also be seen in the higher order bending modes, although those have no stress gradient in the x direction.

|	FEM	Calculations	Error
1 lat	189.88	194.52	-2.39%
1 tor	94.28	89.66	5.16%
2 tor	288.27	268.97	7.18%
3 tor	497.92	448.28	11.07%
4 tor	732.00	627.60	16.64%
1 bend	9.86	9.73	1.41%
2 bend	61.70	60.95	1.22%
3 bend	173.13	170.67	1.44%
4 bend	340.64	334.44	1.85%
5 bend	565.60	552.85	2.31%

The mode shapes can also be shown as part of the results in finite element analysis. Below are several of the mode shapes that are part of the solution.
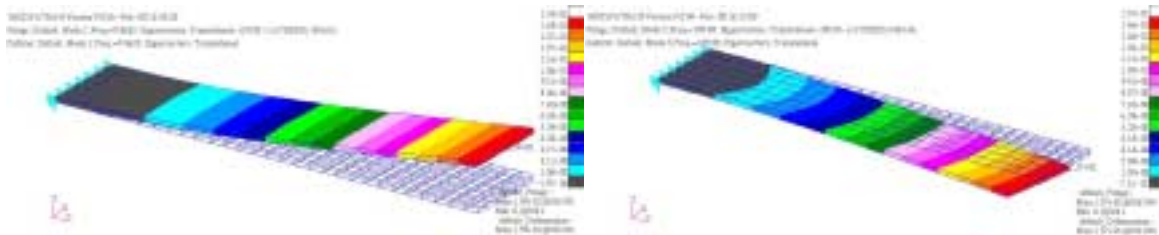
Figure 27. First Bending and First Lateral Bending Modes.
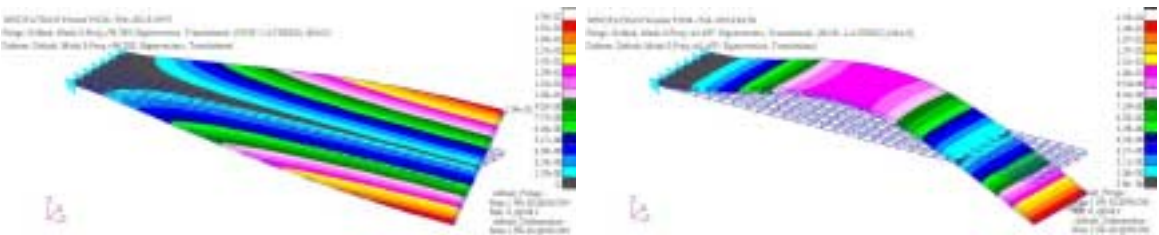
Figure 28. First Torsion and Second Bending Modes.
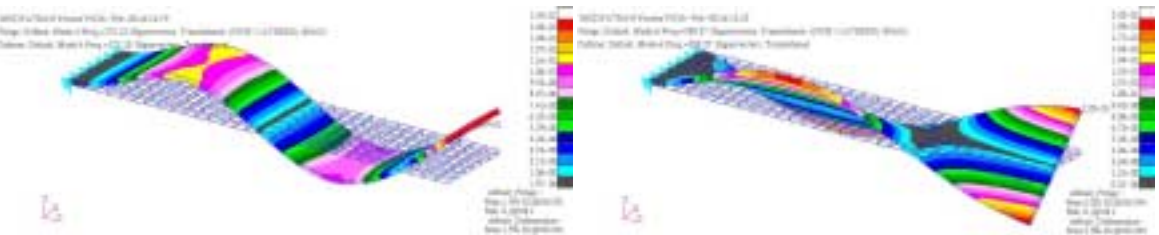
Figure 29. Third Bending and Second Torsion Modes.

These modes compare well to the shapes that were calculated in the theorectical case. The enforcement of the boundary conditions, both the natural and geometric, is clear. The enforcement of the zero displacments and rotations is visible on the root end. The zero curvature (zero moment) condition can be seen in each mode on the free end. It is harder to see the zero shear condition, but

the free face of the beam remains perpendicular to the edges leading to the end face.

6.5   Element Applicability and Meshing Criteria

It is interesting to note that the model run with the shell elements with reduced order integration had more accurate results with fewer elements. This is because the theory of plates is based on the same stress strain relationship that the shell elements use.

Solid elements are much more useful when there is a nonuniform thickness or if there is a dramatic stress gradient through the thickness caused by forces other than bending. It is much easier to correctly vary the thickness of the solid elements along a span than on the shell elements. Additionally, it is possible to put more than a single layer of elements through the thickness unlike in shell elements.

Although the element is no longer as susceptible to being overly stiff, this does not mean that the aspect ratio of the elements does not matter at all. It is still important to keep the brick as close to a perfect cube as practical for a given situation. This is because multiplying the formulation by the determinate of the Jacobian forms the stiffness matrix. If the element is very skewed, this transformation into the local coordinates is not as accurate. To keep the error to a minimum the skew of element must be at a minimum practical level. In our example it would be best to have all elements a cube 0.1 on each edge. This would unnecessarily increase the mesh to 2000 elements. As long as the element edges remain normal the aspect ratio can be left higher than 1.

SECTION 7
BRICK ELEMENT WITH REDUCED INTEGRATION

The final element that we will look at is the brick element with reduced integration. There is no bubble mode, so the element is comparable to the reduced integration shell element. The element still uses the brick element definition of the strain energy.

The same formulations of the strain energy and stress-strain relationship are used. Just as we used a single integration point in the reduced shell integration, there will only be one integration point in each of the local coordinate directions.

Mode shapes are not changed by reduced integration, although the associated eigenvalues are. These new eigenvalues dramatically change the energy required to deform the structure, bringing the solution towards the exact solution.

7.1   Mode Shapes

The reduced order integration technique changes the associated eigenvalues for some mode shapes. These are caused by the modification of the stiffness matrix when reduced order Gauss point integration incorrectly evaluates it. The theory is the same as it is in the shell elements; the changes allow the correct mode to deform with less energy being used by the same deflection.

This theory works, but not as well as in the shell element. The main reason that it is worse than the shell element is that the eigenvalue is reduced to zero instead of some new positive value. Both were similar in that only the bending modes were effected. The goal was to reduce the energy required to excite these modes, so the method worked well in that respect.

7.2   Deflection Solution

The change is apparent in the solution. The solution quickly approaches the closed form solution. An interesting thing happens as the number of elements is reduced to just a couple elements. The zero eigenvalues of the bending modes prevent the stiffness matrix from being inverted. After a few of the elements are connected the complete system can no longer exhibit a single bending mode, so the matrix is no longer singular. The individual elements still have zero energy associated with their bending so the solution will not be exact. All strain energy is based on the other elastic modes although the solution shows primarily bending. The convergence is close to the exact solution, but it is not as close as the bubble mode solution.

If the elements do not converge to the correct solution, they do converge quickly. The difference between 30 spanwise elements (180 total elements) and 50 spanwise elements (500 total) is negligible.
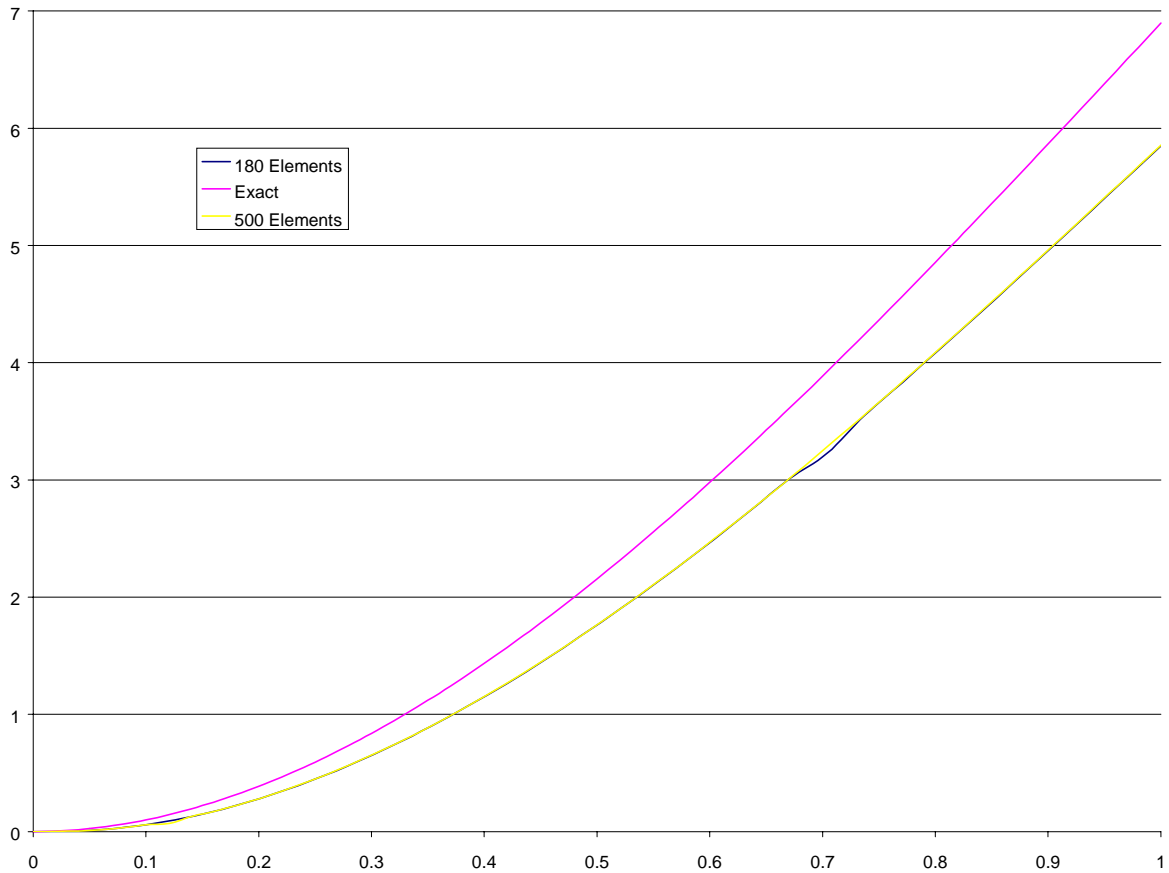
Figure 30. Reduced Integration Defection Solution

7.3   Natural Frequencies

There is also an associated system frequency change with the new elements. Much like the deflection solution, the frequencies come closer to the exact solution, but not as close as the bubble functions. Depending on the application the frequencies may not be close enough to accept. They still have about ten-percent error in the low frequency modes.

	FEM	Calculations	Error
1 lat	190.43	194.52	-2.10%
1 tor	94.88	89.66	5.83%
2 tor	291.17	268.97	8.25%
3 tor	506.14	448.28	12.91%
4 tor	749.94	627.60	19.49%
1 bend	10.59	9.73	8.88%
2 bend	66.16	60.95	8.54%
3 bend	186.05	170.67	9.01%
4 bend	367.41	334.44	9.86%
5 bend	612.33	552.85	10.76%

The error in frequency stems from the same cause as the error in the deflection. The system has the incorrect energy associated with the given deflection modes, changing the amount of energy (frequency) required to excite a given mode.

7.4 Comparison with Bubble Node

The solution is not as accurate as the bubble mode in this solution. That is because instead of making the model more accurate by increasing the order of the shape functions to better enforce the strain displacement relationship, the most prominent deflection mode has the eigenvalue arbitrarily reduced. It does make sense that if a system should bend and it doesn't, reducing energy associated with the bending mode will make the system approach the correct value. The problem is that a better solution comes from the degradation of the model and not from a more exact model.

Another way to look at the solution is to say that the shape functions are a series of normal functions added together. As the number of normal functions increases, the solution approaches the exact solution as in the Fourier Series expansion of a function. It can be shown that increasing the polynomial order of the shape function will bring the solution closer to the exact solution. That is the theory behind p-elements, which increase the order of the polynomial shape function until the solution converges within a given tolerance.

Conversely, the reduced order integration has no proof that the mesh will even converge to the right solution let alone a more accurate one than a fully integrated one. In practice it does converge towards the correct solution most of the time, but the analyst should be aware that there is no guarantee that it will.

The reason that the bending mode eigenvalue goes to zero using reduced integration is that the single Gauss point is at a zero strain position in the element. That means that it will have zero energy and a zero eigenvalue. This can be seen in the figure below.
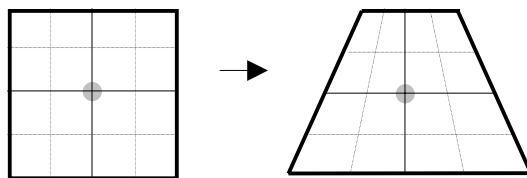
The single Gauss point in the center of the element is located in the middle of symmetric deflection so there is no strain at that point.

Figure 31. Gauss Point Location in Reduced Order Bending Mode.

In the figure you can also see the locations of the fully integrated Gauss points by the intersection of the dashed lines. It is clear that they are on lines that deform, and therefore have an energy associate with that deflection.
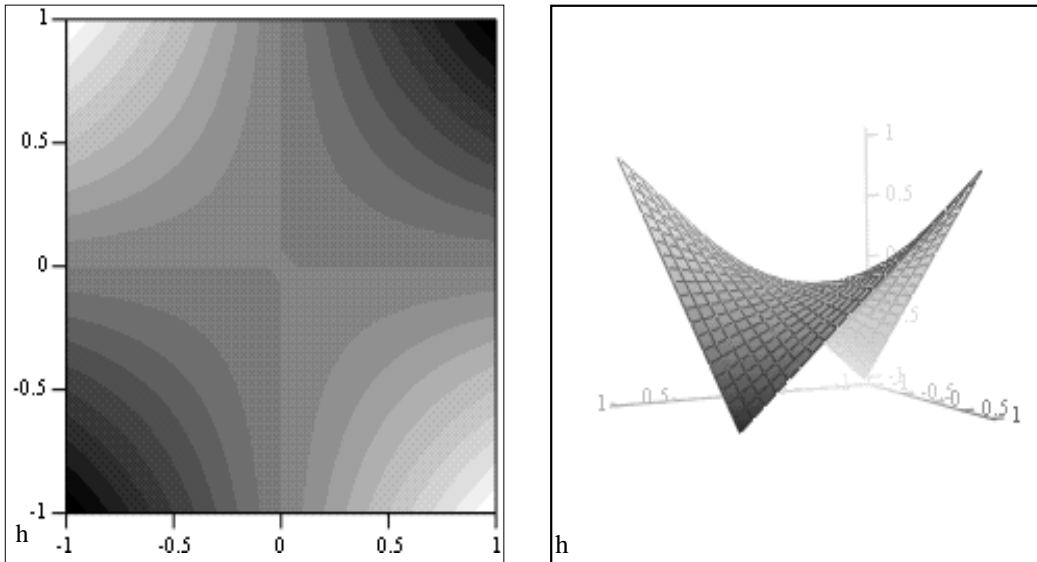
SECTION 8
CONCLUSIONS AND RECOMMENDATIONS

The goal of any structural analysis is to correctly predict the conditions that will exist in a given structure. The best way to accomplish this when using these elements that are subject to being over stiff is to understand what the different element property choices mean mathematically in the model.

The reduced integration technique works well in the shell method because the bending strain definition is:

$$EI(\phi')^2$$

and phi prime is a non-zero constant at the Gauss point. This implies that there will be a non-zero eigenvalue associated with the bending mode because there is strain at the Gauss point.

In the brick element, the Gauss point is at a saddle point. The values of the gradients in both the r and the s directions are zero at the Gauss point, as are the shear gradients. This means that the strain at the Gauss point is zero and will produce a zero eigenvalue. The saddle point can be seen in the figures showing u deflection in a bending mode.

Figure 32. Deflection Plot of Bending Mode Shape.

The main difference is again due to the difference in the strain energy definition. The Cauchy formulation used in the brick element is not accurate in these conditions dominated by bending and shear.

The reduced order shell element is the best solution for overcoming locking in the shell element because the stiffness of the bending mode is not reduced to zero.

It is the best formulation of the element to use in most conditions. The analyst should still be aware that there is still no method to know that the solution that the model converges to is the exact solution, but in most cases it is closer to reality than the fully integrated element.

The best brick element formulation to use is the element that has quadratic shape functions. That means that the simplest element would be the eight-node element using bubble functions. Other elements that also use the quadratic shape functions are the 20, 21, 26, and 27 node elements. These will dramatically increase the computational time if the number of elements remains constant.

Modern FEA code provides hourglass mode stiffening. This is a change in the stiffness matrix that can provide stiffness to those modes that normally would have a zero eigenvalue under reduced integration. This is another solution to the problems associated with reduced integration of brick elements.

Whatever formulation and elements used in the FEM, it is very important that the person using them knows how and why they act as they do. An analysis is only as good as the method used, so knowing that you are using the right method for the particular analysis is extremely important.